Journal of Bangladesh Academy of Sciences, Vol. 35, No. 1, 67-75, 2011

SINTERING TEMPERATURE DEPENDENT PERMEABILITY OF NANOCRYSTALLINE $Ni_{0.20}Cu_{0.30}Zn_{0.50}Fe_2O_4$ FERRITE

M. L .RAHMAN[*1], M. H. R. KHAN[2], S. T. MAHMUD AND
A. K. M. AKTHER HOSSAIN

Department of Physics, Bangladesh University of Engineering and Technology, Dhaka, Bangladesh

ABSTRACT

The spinel ferrite of $Ni_{0.20}Cu_{0.30}Zn_{0.50}Fe_2O_4$ was studied at room temperature using X-ray diffraction pattern prepared by auto combustion technique. The analysis of the XRD patterns showed that the sample has a single phase cubic spinel structure. The bulk density, average grain size and initial permeability increase with increasing sintering temperature up to a optimum temperature. Beyond that temperature all those properties decreases. The value of relative quality factor decreases with increasing sintering temperature. The DC magnetization measurement showed that at room temperature the sample is in ferrimagnetic state. The number of Bohr magneton, $n(\mu_B)$, Néel temperature, T_N, and the field at which saturation occurs were also calculated and possible explanation for the observed characteristics of microstructure, initial permeability, DC magnetization, and Néel temperature of the studied sample are presented.

Key words: Ferrites, Dependent permeability, Nanocrystalline

INTRODUCTION

With the rapid development of mobile communication and information technology, the electronic devices with small size, low cost and high performances are in demand (Qi *et al.* 2002). Recently, surface mounting devices (SMD) have been rapidly developed using multilayer chip inductor (MLCI). Ni-Zn ferrites are widely used in many applications, including MLCI, microwave components and devices (Yan *et al*. 2004, Yue *et al.* 2003). Substitution of copper in these ferrites is known to improve the sintering properties drastically (Nakamura 1997). So there has been a growing interest in *Ni-Cu-Zn* ferrites in producing multilayer type chips mainly because of these materials have a very high permeability, high resistivity and are most suitable for applications at frequencies over 1 MHz. For the application of these ferrites in high frequency devices, the materials should have low losses at high frequencies. The method of preparation of ferrites and the condition of sintering profoundly influence the magnitude of the initial permeability (Kakatkar *et al.* 1996). Depending on the composition and process conditions such as sintering temperature and atmosphere, the lattice site occupancy changes leading to the

[*] Corresponding author: <lutfor_59@yahoo.com>.
[1] Department of Mathematics and Natural Sciences (MNS), BRAC University, Dhaka, Bangladesh.
[2] Department of Arts & Sciences, Ahsanullah University of Science and Technology, Dhaka, Bangladesh.

change in magnetic properties (Singh *et al*. 2002, Rath *et al.* 2002). In addition, for a given cation distribution, the magnetic properties depend strongly on the microstructural features such as morphology, crystallite size and porosity (Mahmud *et al.* 2006, Hossain *et al.* 2007). Magnetic applications, such as computer memory and pulse transformers operating at high frequency, require high resistivity, high saturation magnetization, high Néel temperature and low magnetic losses. In the present work a systematic study of density porosity and initial permeability of $Ni_{0.20}Cu_{0.30}Zn_{0.50}Fe_2O_4$ is undertaken. Structural investigations are also made using x-ray diffraction analysis and high resolution optical microscopy.

EXPERIMENTAL

A sample of $Ni_{0.20}Cu_{0.30}Zn_{0.50}Fe_2O_4$ was prepared through auto combustion method. The stoichiometric amounts of highly pure powders of $Ni(NO_3)_2.3H_2O$, $Cu(NO_3)_2.3H_2O$, $Zn(NO_3)_2.6H_2O$ and $Fe(NO_3)_3.9H_2O$ were dissolved in ethanol. Then the solution was heated at 70°C to transform into gel. The foamy gels are kept on a pre-heated oven at 150°C which caused its spontaneous ignition. The combustion reaction is completed within a few seconds and loose powders are formed. These powders are crushed and ground thoroughly. Then the resultant powders were calcined at 900°C for 5hrs and then pressed uniaxially into disk shaped (about 10 mm outer diameter, 2 - 3 mm thickness) and toroid shaped (about 10 mm outer diameters, 5 mm inner diameter, and 3 mm thickness) samples. This sample was then sintered at 1100, 1150, 1200 and 1250°C for 5 hrs in air atmosphere. The temperature ramps were 10°C/min for heating and 5°C/min for cooling. The bulk densities were measured by Archimede's principle using water. The ferrites were characterized by X-ray diffraction using CuKα radiation. Average grain sizes (grain diameter) of the sample were determined from optical micrographs by linear intercept technique (Hossain 1998).The frequency characteristics of $Ni_{0.20}Cu_{0.30}Zn_{0.50}Fe_2O_4$ ferrite sample i.e. the initial permeability spectra were investigated using a Wayne Kerr Precision Impedance Analyzer (model no. 6520A). The complex permeability measurements on toroid shaped specimens have been carried out at room temperature of the sample in the frequency range 1 KHz - 15MHz. The values of the measured parameters obtained as a function of frequency and the real part (μ') of the complex permeability have been calculated using the following relations: $\mu' = L_s/L_o$, where L_s is the self inductance of the sample core and $L_o = (\mu_o N^2 h/2\pi) \ln(r_o/r_i)$ is derived geometrically, where L_o is the inductance of the winding coil without the sample core, N is the number of turns of the coil (N = 5), h is the thickness, r_o is the outer radius and r_i is the inner radius of the toroidal specimen. The relative quality factor was calculated from the relation: $Q = \mu'/\tan\delta$, where $\tan\delta$ is the loss factor. The DC magnetization measurements was made on pieces of the sample (approximate dimensions 2 ×1 ×1 mm^3) using the SQUID magnetometer (MPMS-5S; Quantum design Co. Ltd.). The temperature-

dependent permeability was measured at a fixed frequency (100 kHz). The Néel temperature, T_N, was calculated from the temperature-dependent permeability measurement.

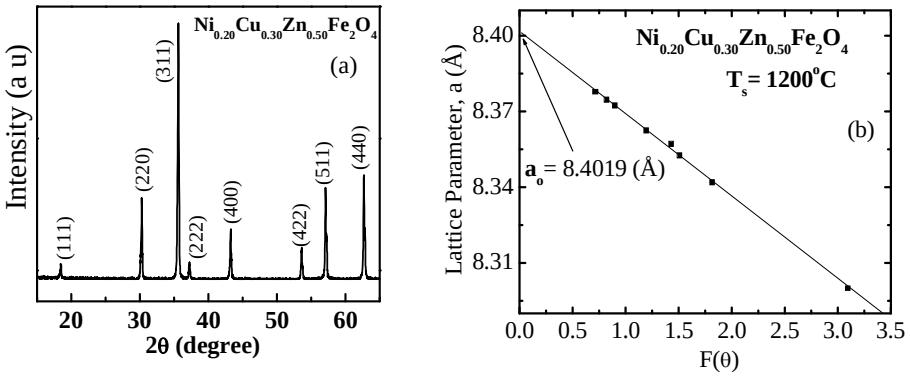

Fig. 1. (a) The X-ray diffraction pattern. (b) The Nelson-Riley function *F(θ)* vs lattice parameter for $Ni_{0.20}Cu_{0.30}Zn_{0.50}Fe_2O_4$.

RESULTS AND DISCUSSION

The X-ray diffraction (XRD) pattern for $Ni_{0.20}Cu_{0.30}Zn_{0.50}Fe_2O_4$ sample is shown in Fig. 1(a). The XRD patterns clearly shows the single phase and formation of spinel structure. Analyzing the XRD patterns authors detect that the positions of the peaks comply with the earlier reported value (Hossain *et al.* 2007). The values of lattice parameter '*a*' of all the peaks for the sample is plotted against Nelson-Riley function, *F(θ)*, in Fig. 1(b). The average crystalline size for the sample evaluated using the major diffraction peak (311) by Debye Scherrer formula (Klug *et al.* 1997) $D = 0.9\lambda/\beta\cos\theta$, where λ is the wavelength of X-ray, θ is the angle of the incident beam in degree and β is the full width at half maximum (FWHM) of the fundamental reflection (311) in radian of the FCC ferrites phase. The average particle size of the sample in the nano particle range of 73 nm. Fig. 2 shows the density and porosity as a function of sintering temperature, T_s. The density of the $Ni_{0.20}Cu_{0.30}Zn_{0.50}Fe_2O_4$ sample increases as the sintering temperature increases from 1100 to 1200°C and above 1200°C the density decreases slightly. On the other hand, porosity (*P)* of the sample decreases, as increasing sintering temperature up to 1200°C, and above 1200°C the porosity increases. The increase in density with sintering temperature is expected. This is because during the sintering process, the thermal energy generates a force that drives the grain boundaries to grow over pores, thereby decreasing the pore volume and denser the material. At higher sintering temperatures the density decreases because the intragranular porosity increases resulting from discontinuous grain growth which is shown in Fig. 3. When the grain growth rate is

very high, pores may be left behind by rapidly moving grain boundaries, resulting in pores that are trapped inside the grains.

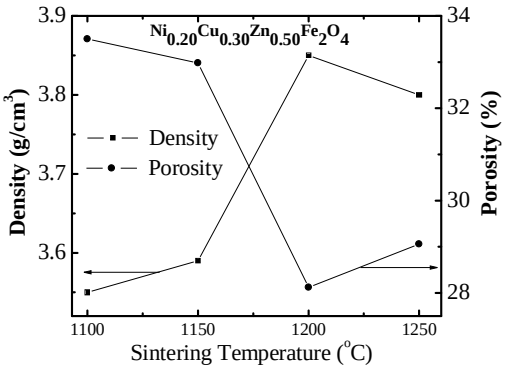

Fig. 2. The variation of bulk density and porosity with sintering temperature for $Ni_{0.20}Cu_{0.30}Zn_{0.50}Fe_2O_4$.

The discontinuous growth of grain rises with temperature and hence, contributing toward the reduction of the bulk density. Such a conclusion is in agreement with that previously reported in case of *NiMnZn* ferrites (Hossain *et al.* 2009).

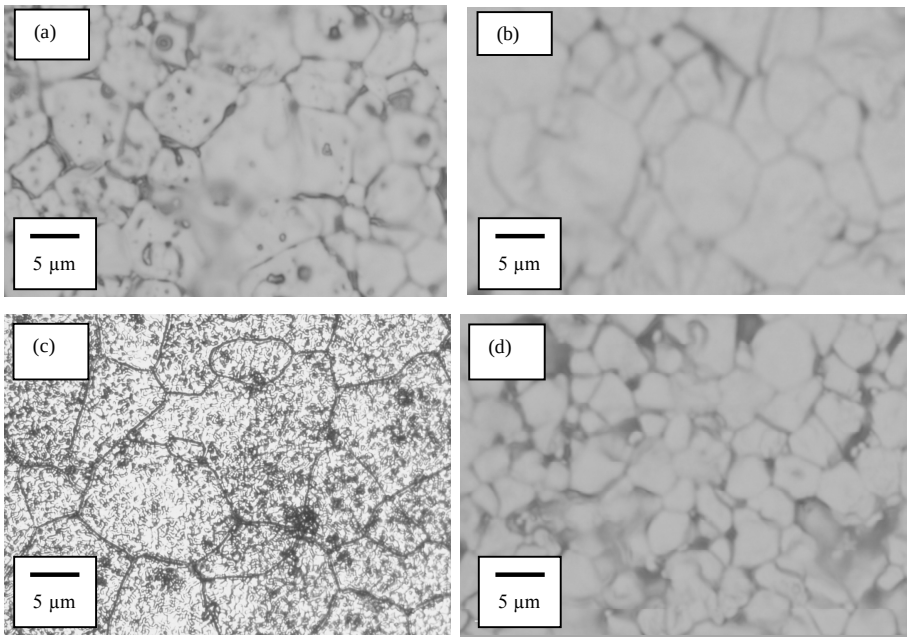

Fig. 3. The optical micrographs of $Ni_{0.20}Cu_{0.30}Zn_{0.50}Fe_2O_4$ sample sintered at (a) 1100°C, (b) 1150°C, (c) 1200°C, (d) 1250°C.

The optical micrographs of $Ni_{0.20}Cu_{0.30}Zn_{0.50}Fe_2O_4$ sintered at different temperature are shown in Fig. 3. The grain size is significantly dependent on sintering temperature. The average grain size increases from 2.04 to 3.12 μm with increasing sintering temperature up to 1200°C. Beyond this temperature grain size decreases. The uniformity in the grain size and the average grain diameter can control materials properties such as the magnetic permeability. The behaviour of grain growth reflects the competition between the driving force for grain boundary movement and the retarding force exerted by pores (Costa *et al.* 2003). When the driving force of the grain boundary in each grain is homogeneous, the sintered body attains a uniform grain size distribution; in contrast, discontinuous grain growth occurs if this driving force is inhomogeneous.

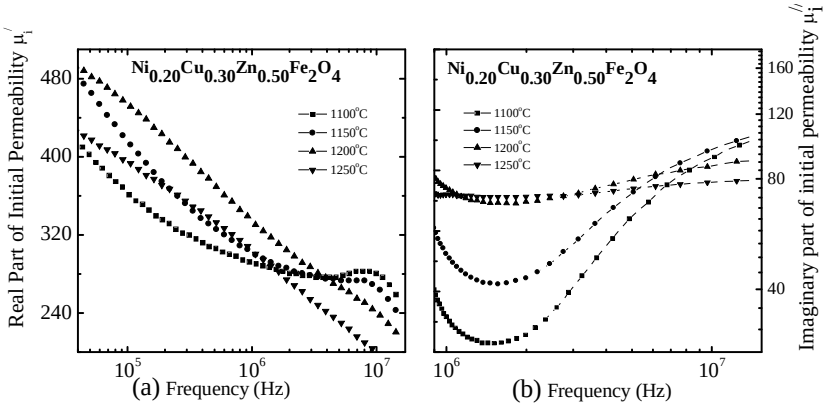

Fig. 4. The variation of (a) μ_i' and (b) μ_i'' spectra for $Ni_{0.20}Cu_{0.30}Zn_{0.50}Fe_2O_4$ samples sintered at different temperatures in air.

Fig. 4 shows the complex initial permeability spectra for $Ni_{0.20}Cu_{0.30}Zn_{0.50}Fe_2O_4$ sample sintered at 1100, 1150, 1200 and 1250°C. It is observed that the real part of initial permeability, μ_i' of $Ni_{0.20}Cu_{0.30}Zn_{0.50}Fe_2O_4$ ferrite increases from 361 to 453 as sintering temperature, T_s increases from 1100 to 1200°C and then decreases.. The variation of μ_i' with frequency for the samples can be explained on the basis of Globus model. According to this model, the relaxation character is $(\mu_i' - 1)^2 f_r = \text{constant}$, where μ_i' is the static initial permeability (Chauhan *et al.* 2004).The initial permeability of ferrite is related by $\mu_i' \propto \frac{M_s^2 D}{\sqrt{K}}$; where M_s is the saturation magnetization, K is the magneto crystalline anisotropy constant and D is the average grain diameter (Chauhan *et al.* 2004). The increase in μ_i' with increasing sintering temperature can be attributed to the increase in grain size, which increases with increasing sintering temperature up to an optimum temperature T_s, as shown in Fig. 3. Increase in grain size results in an increase in the number of domain walls in each grain. As the movement of walls

determines the initial permeability, any increase in the number of domain walls would result in an increase in μ_i'. Thus for a large grain the permeability should increase as it varies proportionally with grain diameter.

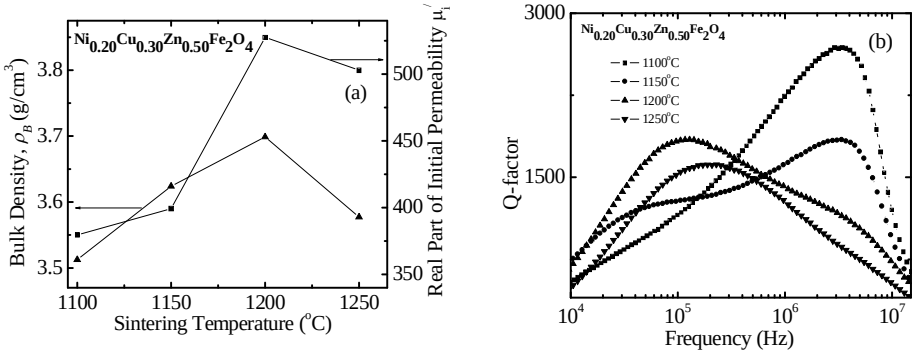

Fig. 5. The variation of (a) μ_i' and ρ_B with T_s and (b) quality factor with frequency for $Ni_{0.20}Cu_{0.30}Zn_{0.50}Fe_2O_4$.

So we can expect higher μ_i' for the samples sintered at higher T_s. However authors observed that μ_i' is found to be maximum at 1200°C (optimum T_s) as shown in Fig. 5(a). If the sintering temperature is higher than that of the optimum T_s, μ_i' decreases due to the effect of grain size. It is possible that the sample sintered at higher temperatures, increase the number of pores within the grain which results decreasein permeability. The pores act as pinning sites for the domain wall movement. Consequently, domain wall movement is restricted and this limits the rate of growth of μ_i'. It is also found that the sintered density is highest for these temperatures, Fig. 5(a). It is also observed that f_r decreases with increase in sintering temperature. As sintering temperature increases, the domain wall relaxation frequency shifted from 3.41 to 0.13 MHz but at higher sintering temperature i.e. 1250°C it increases again to 0.19 MHz. The μ_i' of the sample are found independent of frequency below the relaxation frequency. Since the relaxation frequency of domain wall oscillation is inversely proportional to grain diameter (Goldman 1999), so f_r observed in the present work is expected to shift toward lower frequency with the increase in sintering temperature. Fig. 5(b) shows the variation of relative quality factors, Q with frequency for $Ni_{0.20}Cu_{0.30}Zn_{0.5}Fe_2O_4$ sintered at various temperatures, T_s. The maximum Q value is about 2683 which occurs at T_s = 1100°C. At higher frequencies, Q decreases rapidly. The rapid decrease shows the tendency for a resonance loss peak. It is also observed that Q decrease with the increase in sintering temperature. The Q value depends on the ferrites microstructure, e.g. pores and grain size etc.

Real part of initial permeability, μ_i', as a function of temperature for $Ni_{0.20}Cu_{0.30}Zn_{0.50}Fe_2O_4$ sample sintered at 1250°C is shown in Fig. 6(a). The magnetic transition temperature (T_N) is determined from temperature dependent permeability

measurement which is 166°C. The Néel temperature, T_N, is a function of the magnitude of the exchange energy. Physically, at T_N, the thermal agitation is so violent that it reduces the alignment of the magnetic moment along a given axis to zero (Chauhan *et al*. 2004).

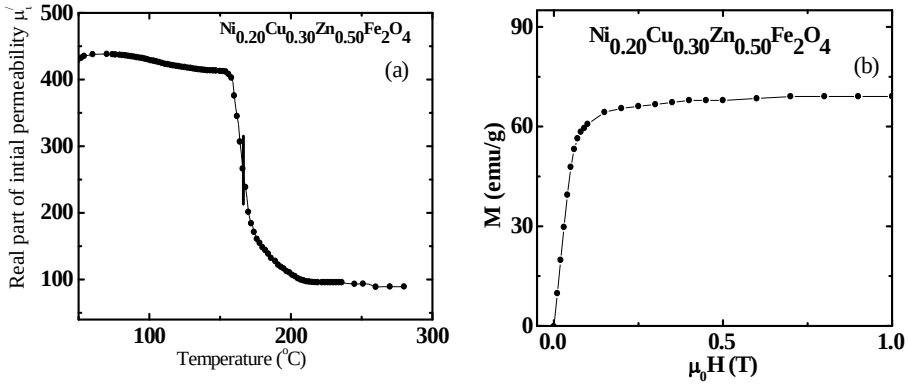

Fig. 6. (a) The temperature dependence of $\mu_i^{/}$ and (b) the M-H curve for $Ni_{0.20}Cu_{0.30}Zn_{0.50}Fe_2O_4$ sample sintered at 1250°C.

It follows that a ferrimagnetic material above its T_N is paramagnetic. Furthermore, it has been shown that the sharpness of the permeability drops at the Néel point can be used as a measure of the degree of compositional homogeneity in the sample. The present $Ni_{0.20}Cu_{0.30}Zn_{0.50}Fe_2O_4$ shows good homogeneity.

The magnetization as a function of applied magnetic field, M(H), for $Ni_{0.20}Cu_{0.30}Zn_{0.50}Fe_2O_4$ sample at room temperature (300 K) is shown in Fig. 6(b). The magnetization of the sample increases linearly with increasing the applied magnetic field up to 0.1 T and attains its saturation value for fields higher than 0.2 Tesla. Therefore, it is clear that at room temperature the sample is in ferrimagnetic state. The saturation magnetization, M_s determined by the extrapolation of the magnetization curve to $\mu_0 H_s = 0$. The value of saturation magnetization, M_s, is 66 emu/g.

The number of Bohr magneton, $n_{\exp}(\mu_B)$, is 2.83 μ_B, was calculated using the relation: $n = \dfrac{M_A \times M_s}{N_A \times 9.27 \times 10^{-21}}$, where M_s is the saturation magnetization and M_A is the molecular weight of the composition. The magnetic moment was theoretically calculated using the possible cation distribution $(Zn_{0.50}Fe_{0.50})[Ni_{0.20}Cu_{0.30}Fe_{1.50}]O_4$, which is equal to 5.70 μ_B. The difference between $n_{th}(\mu_B)$ and $n_{\exp}(\mu_B)$ can be explained by considering the non-collinearity of magnetic moment at octahedral (B) sites which is reflected by the presence of Yafet-Kittle (α_{Y-K}) angle. The value of α_{Y-K} is 49.45°, which have been calculated using the formula $n_{\exp} = (8.5 - x)Cos\alpha_{Y-K} - 2.5$, where $n_{\exp}(\mu_B)$ expressed in the unit of Bohr magneton.

CONCLUSIONS

The bulk density and grain size of ferrite $Ni_{0.20}Cu_{0.30}Zn_{0.50}Fe_2O_4$ increases with increasing sintering temperature up to an optimum sintering temperature, T_s and they would affect magnetic properties directly. The magnetization mechanism of soft magnetic materials like Ni-Cu-Zn ferrite is domain wall motion, which generates high initial permeability due to increase of grain size. Thus it can be concluded that to improve initial permeability by microstructure variation, the ferrites must be sintered at a high temperature. Although pore and grain boundary would obstruct the movement of domain wall. The fewer amount of pores and grain boundary could be obtained at higher sintering temperature and leads to easy movement of domain wall and high initial permeability. With increasing sintering temperature initial permeability of $Ni_{0.20}Cu_{0.30}Zn_{0.50}Fe_2O_4$ ferrite increases by 20%.

ACKNOWLEDGMENTS

The present study was supported by Bangladesh University of Engineering & Technology (BUET).

REFERENCES

Costa, A. C. F. M., E. Tortella, M. R. Morelli and R. H. G. A. Kiminami. 2003. Synthesis, microstructure and magnetic properties of Ni–Zn ferrites. *J. Magn. Magn. Mater*. **256**: 174-182.

Chauhan, B. S., R. Kumar, K. M. Jadhavc and M. Singh. 2004. Magnetic study of substituted Mg–Mn ferrites synthesized by citrate precursor method. *J. Magn. Magn. Mater.* **283**: 71-81.

Goldman, A. 1999. *Handbook of Modern Ferromagnetic Materials.* Kluwer Acad. Pub, Boston, U.S.A.

Hossain, A. K. M., K. K. Kabir, M. Seki, T. Kawai and H. Tabata. 2007. Structural, AC, and DC magnetic properties of $Zn_{1-x}Co_xFe_2O_4$. *J. Phys. Chem. Solids*. **68:** 1933-1939.

Hossain, A. K. M. 1998. Investigation of colossal magnetoresistance in bulk and thick film magnetites. Ph. D. Thesis. Imperial College. London.

Hossain, A. K. M., T. S. Biswas, S. T. Mahmud, T. Yanagida, H. Tanaka and T. Kawai. 2009. Enhancement of initial permeability due to Mn substitution in polycrystalline $Ni_{0.50-x}Mn_xZn_{0.50}Fe_2O_4$. *J. Magn. Magn. Mater*. **321**: 81-87.

Kakatkar, S.V., S. S. Kakatkar, R. S. Patil, A. M. Sankpal, N. D. Chaudhari, P. K. Maskar, S. S. Suryavanshi and S. R. Sawant. 1996. Effect of sintering conditions and Al^{3+} addition on wall permeability in $Ni_{1-x}Zn_xAl_tFe_{2-t}O_4$ ferrites. *J. Mater. Chem. and Phys.* **46:** 96-99.

Klug, H. P. and L. E. Alexander. 1997. X-ray Diffraction Procedures for Polycrystalline and Amorphous Materials. John Wiley& Sons Pub. Co. New York. 637-640.

Mahmud, S. T., A. K. M. Hossain, A. K. M. Abdul Hakim, M. Seki, T. Kawai and H. Tabata. 2006. Influence of microstructure on the complex permeability of spinel type Ni–Zn ferrite. *J. Magn. Magn. Mater*. **305**: 269-274.

Nakamura, T. 1997. Low-temperature sintering of Ni-Zn-Cu ferrite and its permeability spectra. *J. Magn. Magn. Mater.* **168**: 285-291.

Qi, X., J. Zhou, Z. Yue, Z. Gui and L. Li. 2002. Effect of Mn substitution on the magnetic properties of MgCuZn ferrites. *J. Magn. Magn. Mater.* **251**: 316-322.

Rath, C., S. Anand, R. P. Das, K. K. Sahu, S. D. Kulkarni, S. K. Date and N. C. Mishra. 2002. Dependence on cation distribution of particle size, lattice parameter and magnetic properties in nanosize Mn–Zn ferrite. *J. Appl. Phys.* **91**(4): 2211-2215.

Singh, A. K., T. C. Goel, R. G. Mendiratta, O. P. Thakur and C. Prakash. 2002. Magnetic properties of Mn-substituted Ni–Zn ferrites. *J. Appl. Phys.* **92**(7): 3872-3876.

Yan, S., J.Geng, L. Yin and E. Zhou 2004. Preparation of nanocrystalline NiZnCu ferrite particles by sol-gel method and their magnetic properties. *J. Magn. Magn. Mater.* **277**: 84-89.

Yue, Z., Zhou J., Gui Z. and Li L. 2003. Magnetic and electrical properties of low-temperature sintered Mn-doped NiCuZn ferrites. *J. Magn. Magn. Mater.* **264**: 258-263.

(*Received revised manuscript on 18 April, 2011*)